

## RESEARCH ARTICLE

# An all-solid-state NO<sub>3</sub><sup>-</sup> ion-selective electrode with gold nanoparticles solid contact layer and molecularly imprinted polymer membrane

Lei Zhang<sup>1</sup>\*, Zhengying Wei, Pengcheng Liu<sup>1</sup>

State Key Lab for Manufacturing System Engineering, Xi'an Jiaotong University, Xi'an, China

\* These authors contributed equally to this work.

\* [zl870127@stu.xjtu.edu.cn](mailto:zl870127@stu.xjtu.edu.cn)

## Abstract

To improve the single-layer all-solid-state ion selective electrode' defects including poor conductivity of PVC sensitive membrane and interference of water layer between substrate electrode and sensitive membrane, a double-layer all-solid-state ion selective electrode with nanomaterial as the solid contact layer and conductive polymer as the ion sensitive membrane was developed. A gold nanoparticles solid contact layer and a nitrate-doped polypyrrole molecularly imprinted polymer membrane were prepared by electrodeposition. The optimal parameters obtained by electrochemical performance test were 2.5 mmol/L HAuCl<sub>4</sub> electrolyte for solid contact layer and 1800s electrodeposition time for sensitive membrane. The new electrode exhibited a Nernstian response of -50.4 mV/decade and a low detection limit of 5.25×10<sup>-5</sup> mol/L. Potentiometric water layer test showed no water film formed between the gold nanoparticles solid contact layer and nitrate-doped polypyrrole molecularly imprinted polymer membrane. The contact angle between droplet and the surface of solid contact layer was 112.35° and showed good hydrophobic property. Furthermore, the developed electrode exhibited fast response, excellent potential stability and long lifetime. This electrode is suitable for the detection of nitrate concentration in water and liquid fertilizer.

## OPEN ACCESS

**Citation:** Zhang L, Wei Z, Liu P (2020) An all-solid-state NO<sub>3</sub><sup>-</sup> ion-selective electrode with gold nanoparticles solid contact layer and molecularly imprinted polymer membrane. PLoS ONE 15(10): e0240173. <https://doi.org/10.1371/journal.pone.0240173>

**Editor:** Jie Zheng, University of Akron, UNITED STATES

**Received:** May 25, 2020

**Accepted:** September 21, 2020

**Published:** October 15, 2020

**Copyright:** © 2020 Zhang et al. This is an open access article distributed under the terms of the [Creative Commons Attribution License](https://creativecommons.org/licenses/by/4.0/), which permits unrestricted use, distribution, and reproduction in any medium, provided the original author and source are credited.

**Data Availability Statement:** All relevant data are within the paper.

**Funding:** The financial support is provided by the National Key Research and Development Plan of China (No.2017YFD0201500).

**Competing interests:** The authors declare no conflict of interest.

## Introduction

The extensive mode of industrial and agricultural development has led to serious environmental problems [1] including water pollution caused by heavy metals and soil acidification induced by fertilizer accumulation [2]. The concentration determination of heavy metals and fertilizer elements is very important and various techniques have been utilized for the detection. Nie P, et al. [3] used infrared sensor to detect soil nitrogen content and improved the accuracy with partial least square method. Liu Y [4] analyzed the major and trace elements of anhydrous minerals by inductively coupled plasma mass spectrometry (ICP-MS). Keyvan AV and Jafar M [5] developed a farmer-assistant robot to collect the image of crop leaves and

distinguish the extent of nitrogen deficiency by color difference. Other methods for analysis of heavy metals and fertilizer elements include ultraviolet spectrophotometry [6], gas chromatography [7] and liquid chromatography [8]. These spectrometry methods exhibit the drawbacks such as complex pretreatment, expensive instruments and long-term detection and analysis so their applications are restricted to a certain extent.

Ion-selective electrodes (ISEs) based on electrochemical principle are the most frequently used due to its inherent advantages such as portability, low cost, simple operation, low-energy consumption and short-period detection [9]. The traditional liquid-contact ISEs need to be improved because the filling liquid should be replenished regularly and the internal reference electrode Ag/AgCl is oxidized easily [10]. Therefore, the all-solid-state ISEs (ASS-ISEs) have been researched extensively. The coated wire electrodes (CWEs) [11, 12] are the initial form of ASS-ISEs, wherein a thin polymeric film with electroactive materials is coated directly onto a conductor such as platinum wire and graphite rod. However, such an electrode always displays low potential stability on account of the “blocking” interface between the electronically conductive substrate and ion sensitive membrane [13]. The introduction of conductive polymers (CPs, containing polythiophene, polyaniline, polypyrrole and polyparaphenylene) as an internal ion-to-electron layer has improved the potential stability by unblocking the charge transfer at electrode’s interfaces [14–17]. Nevertheless, the inevitable water layer and oxidation reaction with dissolved oxygen between the CPs and ion sensitive membrane limit the practical application of electrodes modified with CPs-type membranes.

Recently, carbon-based nanomaterials and synthetic nanomaterials used as the solid contact layer due to their excellent conductivity and hydrophobicity have been proven effective [18]. Zeng X [19], by means of hydrothermal synthesis, developed three-dimensional molybdenum disulfide nanoflower, which was used as the solid contact layer of K<sup>+</sup> ASS-ISE. Li J [20] utilized the crosslinked three-dimensional porous graphene-mesoporous platinum nanoparticle composite as the solid contact layer of Cd<sup>2+</sup> ASS-ISE, it showed that no water layer existed. The carbonate ion selective electrodes of multi-walled carbon nanotubes as the inner ion-to-electron transducer exhibited good CO<sub>3</sub><sup>2-</sup>-selectivity in environmental monitoring, and several anions selective electrodes (including NO<sub>3</sub><sup>-</sup>, NO<sub>2</sub><sup>-</sup> and H<sub>2</sub>PO<sub>4</sub><sup>-</sup>) were developed [21]. When the electrosynthesis polypyrrole/zeolite composite was employed as solid contact layer in K<sup>+</sup> ASS-ISE, its electrochemical stability and sensitive performance were improved [22]. Although the carbon-based nanomaterials improved the performance of electrodes, the preparation of carbon-based nanomaterials was complex, dangerous and time-consuming. Most researchers adopted drop-coating process to attach the carbon-based nanomaterials on the surface of substrate electrodes, but the solid contact layer was easy to fall off. These influenced the application of carbon-based nanomaterials in ISEs.

The diameter of gold nanoparticles (AuNPs) is 1~100nm, receiving much attention due to its unique properties such as high electron density and surface chemical activity. Its excellent controllable particle size characteristics have important research and practical application value in the field of potentiometric sensors [23–25]. Bhawan N, et al. fabricated a DNA sensor by stamping of layered rGO and rGO/gold nanoparticles/single stranded DNA (rGO/AuNPs/ssDNA) composites over PET substrates [26]. Liang P, et al. utilized dithiothreitol to fine-tune the surface coverage of oligonucleotide-modified AuNPs for perform cocaine detection in 50% urine [27]. AuNPs formed in-situ on a polymer inclusion membrane (AuNPs-PIM) used as a biocompatible sensing platform for bioreceptor conjugation and the signal-output amplification was implemented on the AuNPs-PIM in a label free biosensor [28]. However, AuNPs were mostly used for in-situ labeling of biomedical sensors and rarely applied in ISEs. The composites composed of AuNPs and carbon-based nanomaterials [29] or AuNPs derivatives were used as the ion-to-electron transducers of ISEs, which increased the complexity of

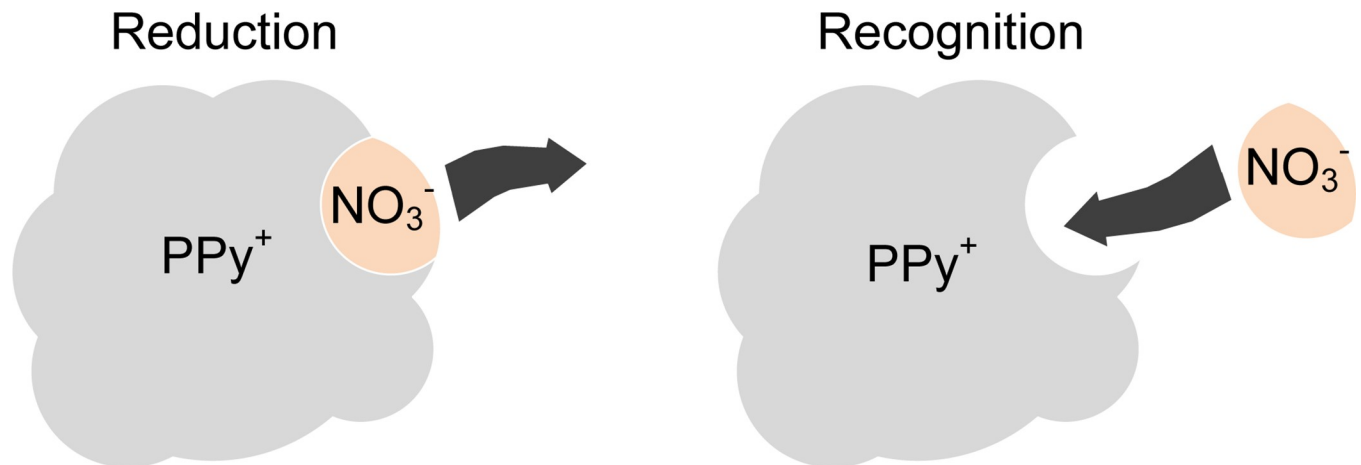


**Fig 1.** PPy-NO<sub>3</sub><sup>-</sup> membrane for selective recognition of NO<sub>3</sub><sup>-</sup>.

<https://doi.org/10.1371/journal.pone.0240173.g001>

preparation. In order to simplify the preparation process, we utilized AuNPs as the solid contact layer in the NO<sub>3</sub><sup>-</sup> ASS-ISE.

A great number of ion-sensitive membranes were plastic films prepared by volatilizing solution in which ionophores and polyvinyl chloride (PVC) were dissolved [30–32]. If the PVC content was less, the ion sensitive membrane was thin and easy to crack. On the contrary, the conductivity of ion sensitive membrane was poor, which affected the ion transmission efficiency. The drop-coating process would also affect the uniformity of ion sensitive membrane. Hence, new materials and technologies are still highly demanded for the development of stable ASS-ISEs.

Selective recognition of the target ions based on "molecularly imprinted" technology provides a new method for preparing sensitive membranes [33]. In the process of electrochemical p-doping polymerization of pyrrole monomer, the positive charge in the generated polymer structure must combine with the negative charge to keep electrically neutral. Therefore, NO<sub>3</sub><sup>-</sup> with negative charge will be doped into the polypyrrole molecular chain generated by polymerization, forming a corresponding physical space. The specific physical space is "molecularly imprinted key" for the specific recognition of NO<sub>3</sub><sup>-</sup>. The principle of nitrate recognition in the sensitive membrane formed through nitrate-doped polypyrrole (PPy-NO<sub>3</sub><sup>-</sup>) is shown in Fig 1. High-performance PPy-NO<sub>3</sub><sup>-</sup> membrane can be obtained by electrodeposition. To sum up, the AuNPs solid contact layer and PPy-NO<sub>3</sub><sup>-</sup> sensitive membrane provide a low-cost and simple method for the preparation of novel high-performance NO<sub>3</sub><sup>-</sup> ASS-ISE.

## Experimental

### Materials and reagents

Glassy carbon electrode (GCE), Ag/AgCl electrode and platinum wire electrode were purchased from Xuzhou Zhenghao Electronics Co., Ltd. Sodium nitrate (NaNO<sub>3</sub>, 99.5% purity), potassium ferricyanide (K<sub>3</sub>[Fe(CN)<sub>6</sub>], 99.5% purity), potassium chloride (KCl, 99.5% purity), pyrrole monomer (99.0% purity), sodium chloride (NaCl, 99.5% purity), potassium phosphate (K<sub>3</sub>PO<sub>4</sub>, 99.0% purity), sodium bromide (NaBr, 99.9% purity), magnesium sulfate anhydrous (MgSO<sub>4</sub>, 99.0% purity) and anhydrous ethanol (99.7% purity) were purchased from Aladdin. Chloroauric acid (HAuCl<sub>4</sub>) solution was of analytical reagent grade from Sinopharm Chemical Reagent Co., Ltd. Deionized water was used throughout.

## Apparatus

Open circuit potential and cyclic voltammetry curve were tested using an electrochemical workstation (PARSTAT 3000, Ametek, U.S.). Solid contact layer and sensitive membrane were electrodeposited by this workstation. Contact angle (CA) between the droplet and the surface of material was measured using an optical contact angle measuring instrument (OCA20, Data-physics, German). A field-emission scanning electron microscope (FESEM, HITACHI, SU8000) was utilized to characterize the morphology of polymer.

## Electrode preparation

Glassy carbon electrode (GCE, 3mm diameter) was polished with 0.5 $\mu$ m alumina powder and then washed ultrasonically in ethanol (the volume ratio of anhydrous ethanol to deionized water was 1:1) and deionized water. In 1 mmol/L K<sub>3</sub>[Fe(CN)<sub>6</sub>] solution the cycle voltammetry curve (scan potential -0.1V~0.6V, scan rate 50 mV/s) was tested. After a pair of reversible redox peaks appeared and the potential difference between the oxidation and deoxidization peak was less than 80 mV, solid contact layer (AuNPs) was electrodeposited on GCE (AuNPs/GCE) with 2.5 mmol/L HAuCl<sub>4</sub> by cyclic voltammetry (scan potential -0.9V~0.3V, scan circle 50, scan rate 50 mV/s). AuNPs/GCE was washed and dried. In the mixture of 0.5 mol/L pyrrole monomer and 0.01 mol/L NaNO<sub>3</sub>, PPy-NO<sub>3</sub><sup>-</sup> membrane was electrodeposited on AuNPs/GCE (PPy/AuNPs/GCE NO<sub>3</sub><sup>-</sup> ASS-ISE) (Fig 2 left) by constant voltage method with 0.7V. For comparison, NO<sub>3</sub><sup>-</sup> ASS-ISE without Au NPs layer (denoted as PPy/GCE NO<sub>3</sub><sup>-</sup> ASS-ISE) (Fig 2 right) was obtained by covering GCE with the above NO<sub>3</sub><sup>-</sup> sensitive membrane. All prepared

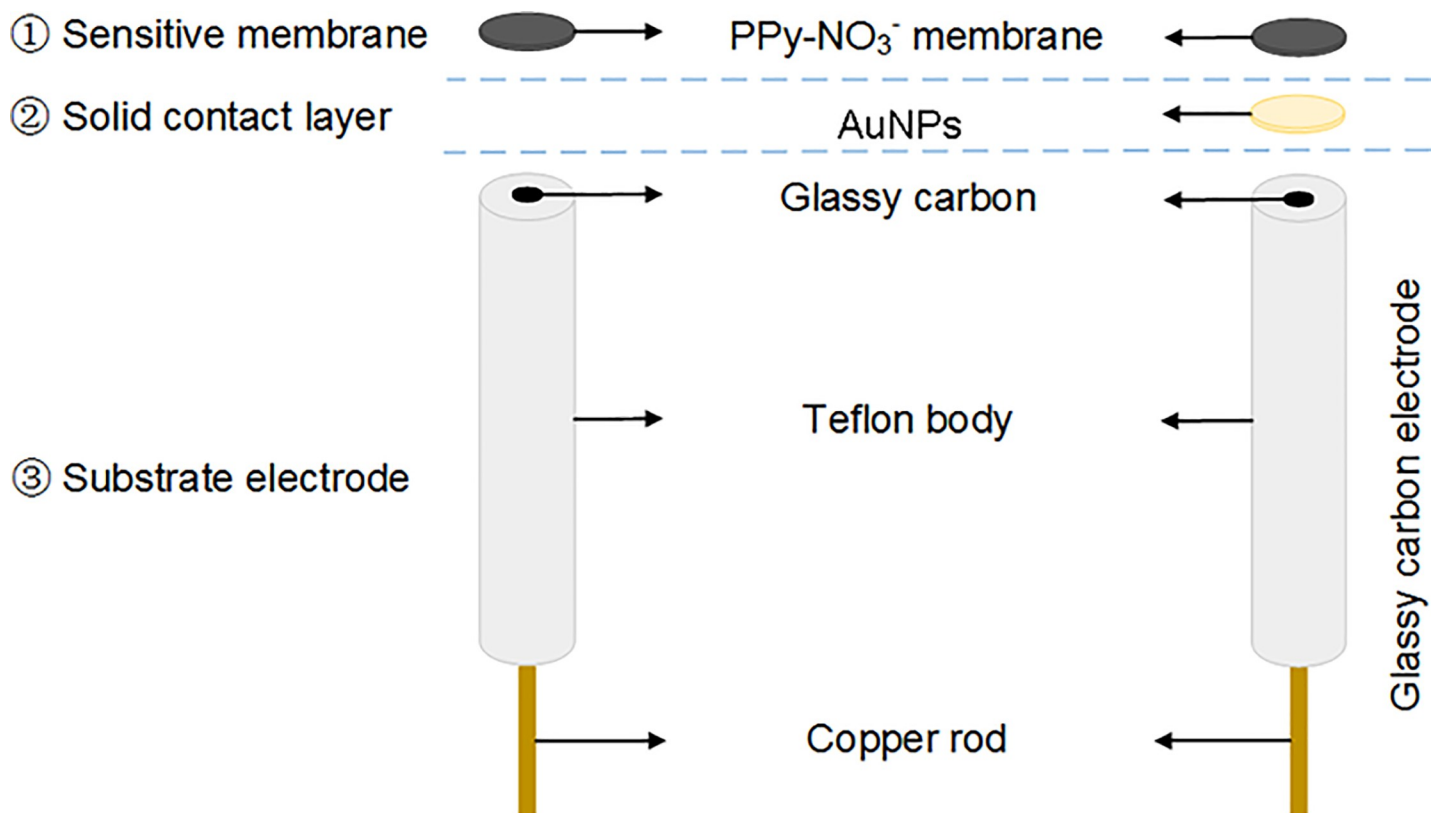


**Fig 2. Schematic of NO<sub>3</sub><sup>-</sup> ASS-ISE: (left) PPy/GCE and (right) PPy/AuNPs/GCE.**

<https://doi.org/10.1371/journal.pone.0240173.g002>

electrodes were washed and left to dry for 12 hours at room temperature (25±1 °C). Then they must be activated in 0.01 mol/L NaNO<sub>3</sub> solution for at least one day.

## Results and discussion

### Potential response of NO<sub>3</sub><sup>-</sup> ASS-ISE

The volume content of sensitive membrane has great influence on the identification efficiency for NO<sub>3</sub><sup>-</sup>. Different membrane thickness can be formed under different time of electrodeposition. In the three-electrode system with GCE as the working electrode, Ag/AgCl as the reference electrode and platinum wire electrode as the counter electrode, electrodeposition in the mixture of 0.5 mol/L pyrrole monomer and 0.01 mol/L NaNO<sub>3</sub> was performed for 600s, 1200s, 1800s, 2400s, 3000s and 3600s. After the fabricated PPy/GCE NO<sub>3</sub><sup>-</sup> ASS-ISE was cleaned and activated, the potential response was measured in the NO<sub>3</sub><sup>-</sup> solution of gradient concentration.

Fig 3(A) shows that the electromotive forces (EMFs) of 6 PPy/GCE NO<sub>3</sub><sup>-</sup> ASS-ISEs have significant changes in NO<sub>3</sub><sup>-</sup> solutions of different concentrations varying from 10<sup>-6</sup> to 10<sup>-1</sup> mol/L, demonstrating these ISEs have good NO<sub>3</sub><sup>-</sup>-sensitivity. At low concentrations, the EMF of each ISE increases slowly under the condition of concentration change and then reaches its stable value. On the contrary, the EMF quickly reaches a stable value at high concentrations. These can be expressed intuitively in response time. In Fig 3(B), the stable EMF of each ISE in 10<sup>-6</sup> mol/L solution are basically equal to that in 10<sup>-5</sup> mol/L solution. At high concentrations, the stable EMF in each concentration shows a decreasing trend with approximate difference, which is in accord with Nernst equation [34]. Hence, the Nernstian response slope (NRS) obtained by data fitting. The lowest concentration in the range of the Nernstian linear response is the lower detection limit (LDL) [35] and the LDL could be calculated from the intersection of the two fitting lines (the inset in Fig 3(B)). The NRSs and LDLs of 6 ISEs are recorded in Table 1. The 3 electrodes electrodeposited with 1200s, 1800s and 2400s have higher detection accuracy and wider working scope because of their larger NRSs and smaller LDLs. Furthermore, the response times of the 3 electrodes in the linear range of concentrations were compared (Fig 4). The comprehensive property of electrode with electrodeposition of 1800s is best, which includes a NRS of -46.7 mV/decade (R<sup>2</sup> = 0.9912) across a working range of 5.37\*10<sup>-5</sup> ~10<sup>-1</sup> mol/L and an average response time of 6.875s. The “-” in NRS represents anion.

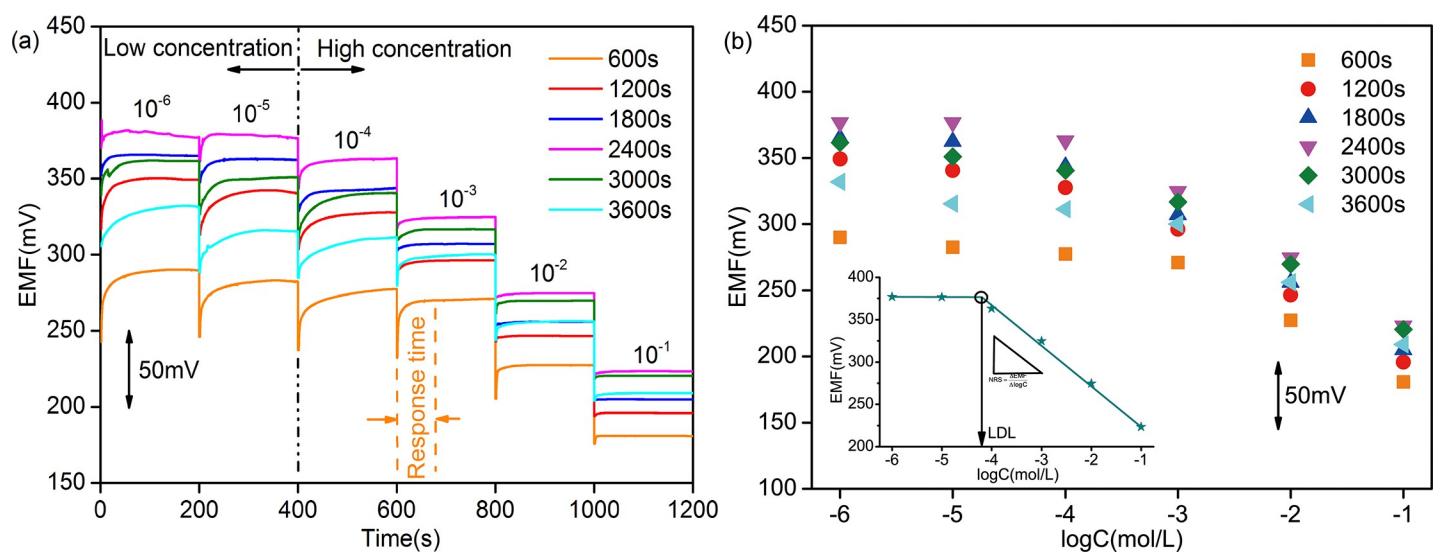


**Fig 3.** EMF measurement of PPy/GCE NO<sub>3</sub><sup>-</sup> ASS-ISE: (a) in NO<sub>3</sub><sup>-</sup> solution of increasing concentration and (b) in stable state. All the electrodes were activated in 0.01 mol/L NaNO<sub>3</sub> solution.

<https://doi.org/10.1371/journal.pone.0240173.g003>

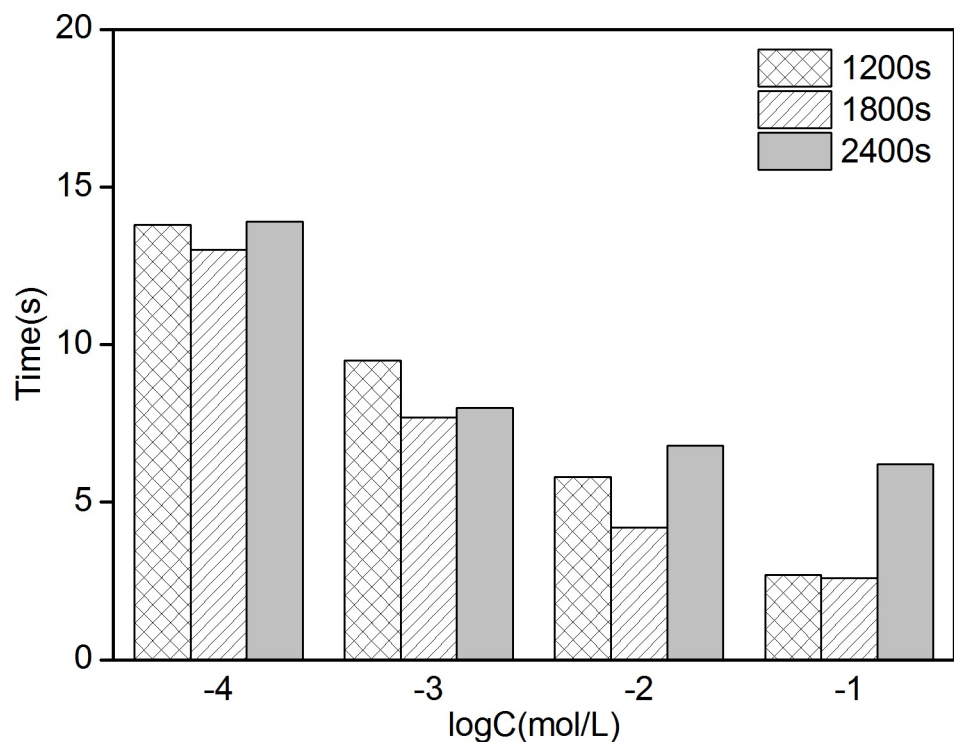
**Table 1.** The Nernstian response slopes and lower detection limits for 6 PPy/GCE electrodes at the concentration range of 10<sup>-4</sup>~10<sup>-1</sup>(mol/L).

| Electrodeposition time(s) | 10 <sup>-4</sup> ~10 <sup>-1</sup> (mol/L) |                       |
|---------------------------|--|-----------------------|
|                           | NRS (mV/decade)                            | LDL (mol/L)           |
| 600                       | -33.4±1.2                                  | 3.55×10 <sup>-4</sup> |
| 1200                      | -44.6±0.9                                  | 1.70×10 <sup>-4</sup> |
| 1800                      | -46.7±0.8                                  | 5.37×10 <sup>-5</sup> |
| 2400                      | -47.0±1.0                                  | 6.31×10 <sup>-5</sup> |
| 3000                      | -40.7±1.5                                  | 1.82×10 <sup>-4</sup> |
| 3600                      | -35.1±1.4                                  | 1.66×10 <sup>-3</sup> |

<https://doi.org/10.1371/journal.pone.0240173.t001>

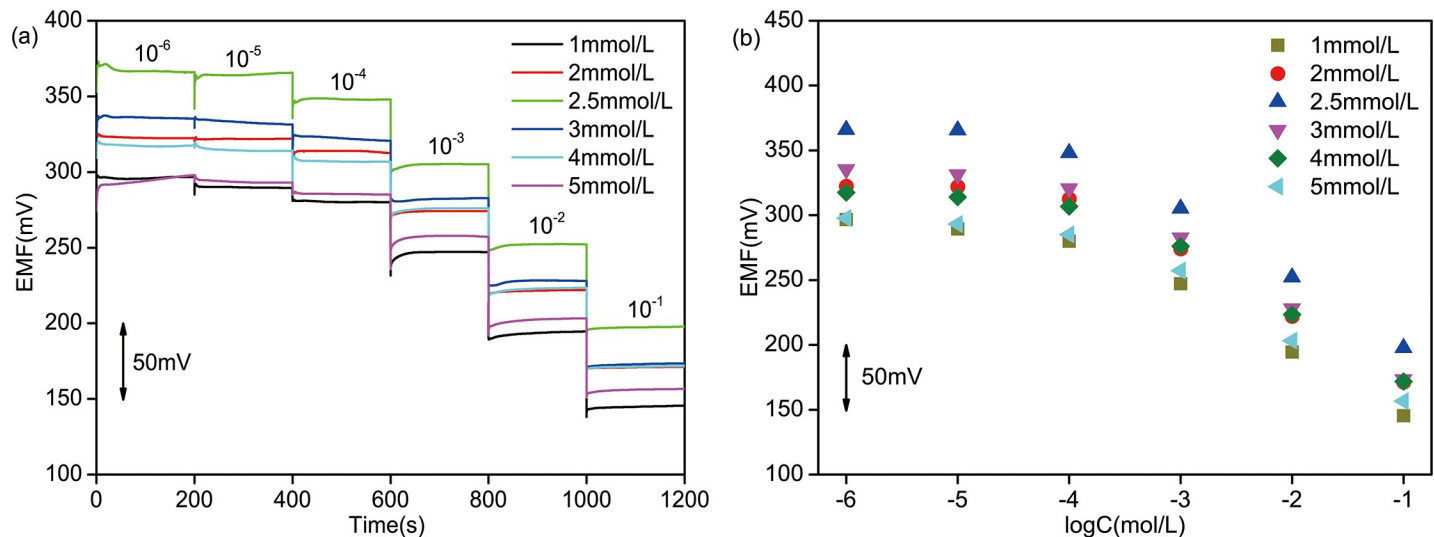
For improving the performance of PPy/GCE NO<sub>3</sub><sup>-</sup> ASS-ISE, a solid contact layer was modified between GCE and PPy-NO<sub>3</sub><sup>-</sup> sensitive membrane. In the three-electrode system, the gold electrodeposition in the electrolyte of HAuCl<sub>4</sub> solution with 1 mmol/L, 2 mmol/L, 2.5 mmol/L, 3 mmol/L, 4 mmol/L and 5 mmol/L was performed to form AuNPs/GCE. Then PPy-NO<sub>3</sub><sup>-</sup> sensitive membrane was electrodeposited on AuNPs/GCE with 1800s. After the fabricated PPy/AuNPs/GCE NO<sub>3</sub><sup>-</sup> ASS-ISE was cleaned and activated, the potential response was measured in the NO<sub>3</sub><sup>-</sup> solution of gradient concentration.

Fig 5(A) shows that the EMF variation trends of 6 PPy/AuNPs/GCE ISEs are the same as that of PPy/GCE ISEs in both low and high concentration solutions. The potential difference of PPy/AuNPs/GCE ISE is larger than that of PPy/GCE ISE at high concentration as shown in Fig 5(B). NRSs and LDLs calculated by the aforementioned method are shown in Table 2. From the three indexes including NRS, LDL and response time (Fig 6), it can be got that the performance of

**Fig 4.** Response times of PPy/GCE NO<sub>3</sub><sup>-</sup> ASS-ISE in the linear range of concentrations.

<https://doi.org/10.1371/journal.pone.0240173.g004>





**Fig 5.** EMF measurement of PPy/AuNPs/GCE NO<sub>3</sub><sup>-</sup> ASS-ISE: (a) in NO<sub>3</sub><sup>-</sup> solution of increasing concentration and (b) in stable state. All the electrodes were activated in 0.01 mol/L NaNO<sub>3</sub> solution.

<https://doi.org/10.1371/journal.pone.0240173.g005>

PPy/AuNPs/GCE with gold electrodeposition in 2.5 mmol/L HAuCl<sub>4</sub> solution is optimal. Compared with PPy/GCE, the average response time decreases by 6.425s and the NRS increases by 7.97%. Hence, the introduction of AuNPs solid contact layer can promote the property of ISE.

### Selectivity of the NO<sub>3</sub><sup>-</sup> ASS-ISE

In order to gauge the response of the ASS-ISE, the selectivity of PPy/GCE and PPy/AuNPs/GCE towards NO<sub>3</sub><sup>-</sup> in solutions containing different anions were investigated. The potentiometric selectivity coefficients ( $K_{ij}^{pot}$ ) of ISEs were determined by the bi-ionic potentials method. The results are summarized in Table 3. It can be seen that the ISEs fabricated in this study have excellent selectivity for NO<sub>3</sub><sup>-</sup>, and their performance was not affected by the presence of Cl<sup>-</sup>, Br<sup>-</sup>, SO<sub>4</sub><sup>2-</sup> or PO<sub>4</sub><sup>3-</sup> ions.

### The micrograph of the polymer

The morphology of PPy-NO<sub>3</sub><sup>-</sup> and AuNPs/PPy-NO<sub>3</sub><sup>-</sup> were characterized by FESEM and the typical images are presented in Fig 7. A panoramic picture shown in Fig 7(A) and Fig 7(C) clearly portrays that the morphology of AuNPs and polymer. A higher resolution images are

**Table 2.** The Nernstian response slopes and lower detection limits for 6 PPy/AuNPs/GCE electrodes at the concentration range of 10<sup>-4</sup>~10<sup>-1</sup>(mol/L).

| HAuCl <sub>4</sub> concentration(mmol/L) | 10 <sup>-4</sup> ~10 <sup>-1</sup> (mol/L) |                       |
|--|--|-----------------------|
|  | NRS(mV/decade)                             | LDL<br>(mol/L)        |
| 1  | -45.7±1.6                                  | 1.20×10 <sup>-4</sup> |
| 2  | -47.6±0.8                                  | 7.76×10 <sup>-5</sup> |
| 2.5                                      | -50.9±1.0                                  | 5.25×10 <sup>-5</sup> |
| 3  | -49.6±1.2                                  | 9.12×10 <sup>-5</sup> |
| 4  | -45.8±1.0                                  | 1.15×10 <sup>-4</sup> |
| 5  | -44.0±1.3                                  | 1.78×10 <sup>-4</sup> |

<https://doi.org/10.1371/journal.pone.0240173.t002>

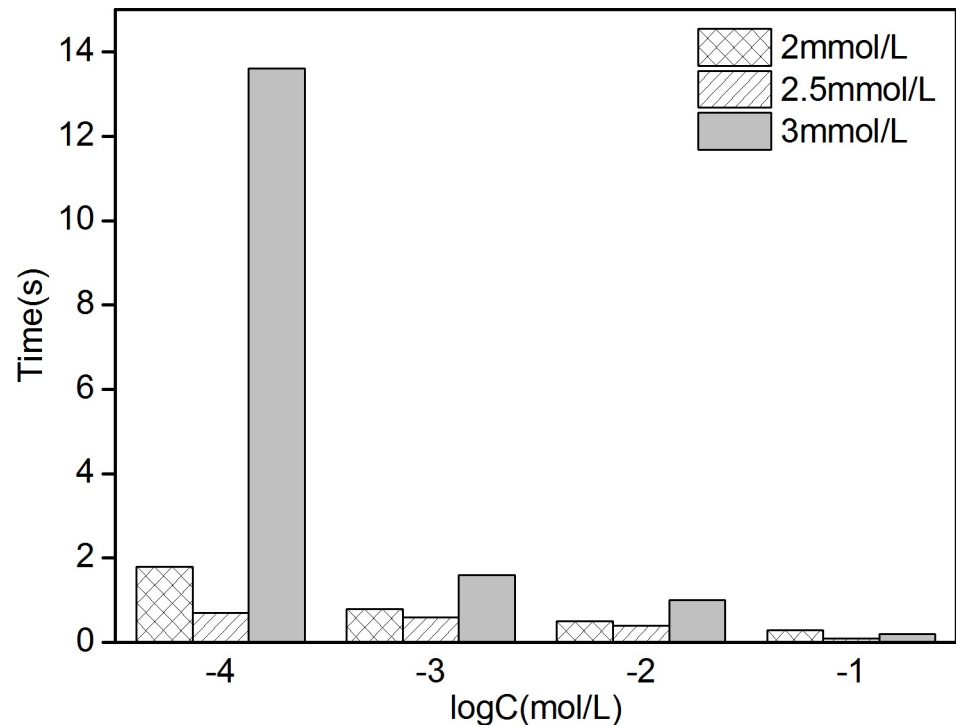


**Fig 6. Response times of PPy/AuNPs/GCE NO<sub>3</sub><sup>-</sup> ASS-ISE in the linear range of concentrations.**

<https://doi.org/10.1371/journal.pone.0240173.g006>

exhibited in Fig 7(B) and Fig 7(D). AuNPs were evenly distributed and PPy looked like cauliflower.

### Water layer test

Polypyrrole is a hydrophilic polymer [36, 37]. Water molecules can easily pass through the PPy sensitive membrane and form a water layer between the GCE and sensitive membrane, which will affect the performance of the electrode prominently. A droplet was placed on the surface of the PPy sensitive membrane and AuNPs solid contact layer to test the contact angle (CA) (the inset in Fig 8). When the CA is less than 90°, the material has strong hydrophilicity. The hydrophobicity enhances with the CA exceeding 90°. The CA of AuNPs solid contact layer is nearly twice that of PPy selectivity membrane as shown in Fig 8, so as to change hydrophilicity to hydrophobicity.

As displayed in Fig 9, PPy/GCE and PPy/AuNPs/GCE were immersed in 0.1 mol/L NaNO<sub>3</sub> solution for half an hour, and the EMFs obtained were stable. When the two electrodes were transferred into 0.1 mol/L NaCl solution, the EMFs of both electrodes changed suddenly. At

**Table 3. Potentiometric selectivity coefficients of PPy/GCE and PPy/AuNPs/GCE NO<sub>3</sub><sup>-</sup> ASS-ISE.**

| Interfering ion               | $K_{ij}^{pot}$       |                      |
|-------------------------------|----------------------|----------------------|
|                               | PPy/GCE              | PPy/AuNPs/GCE        |
| Cl <sup>-</sup>               | $3.1 \times 10^{-2}$ | $2.9 \times 10^{-2}$ |
| Br <sup>-</sup>               | $1.4 \times 10^{-1}$ | $1.1 \times 10^{-1}$ |
| SO <sub>4</sub> <sup>2-</sup> | $6.1 \times 10^{-4}$ | $5.8 \times 10^{-4}$ |
| PO <sub>4</sub> <sup>3-</sup> | $6.4 \times 10^{-5}$ | $6.2 \times 10^{-5}$ |

<https://doi.org/10.1371/journal.pone.0240173.t003>



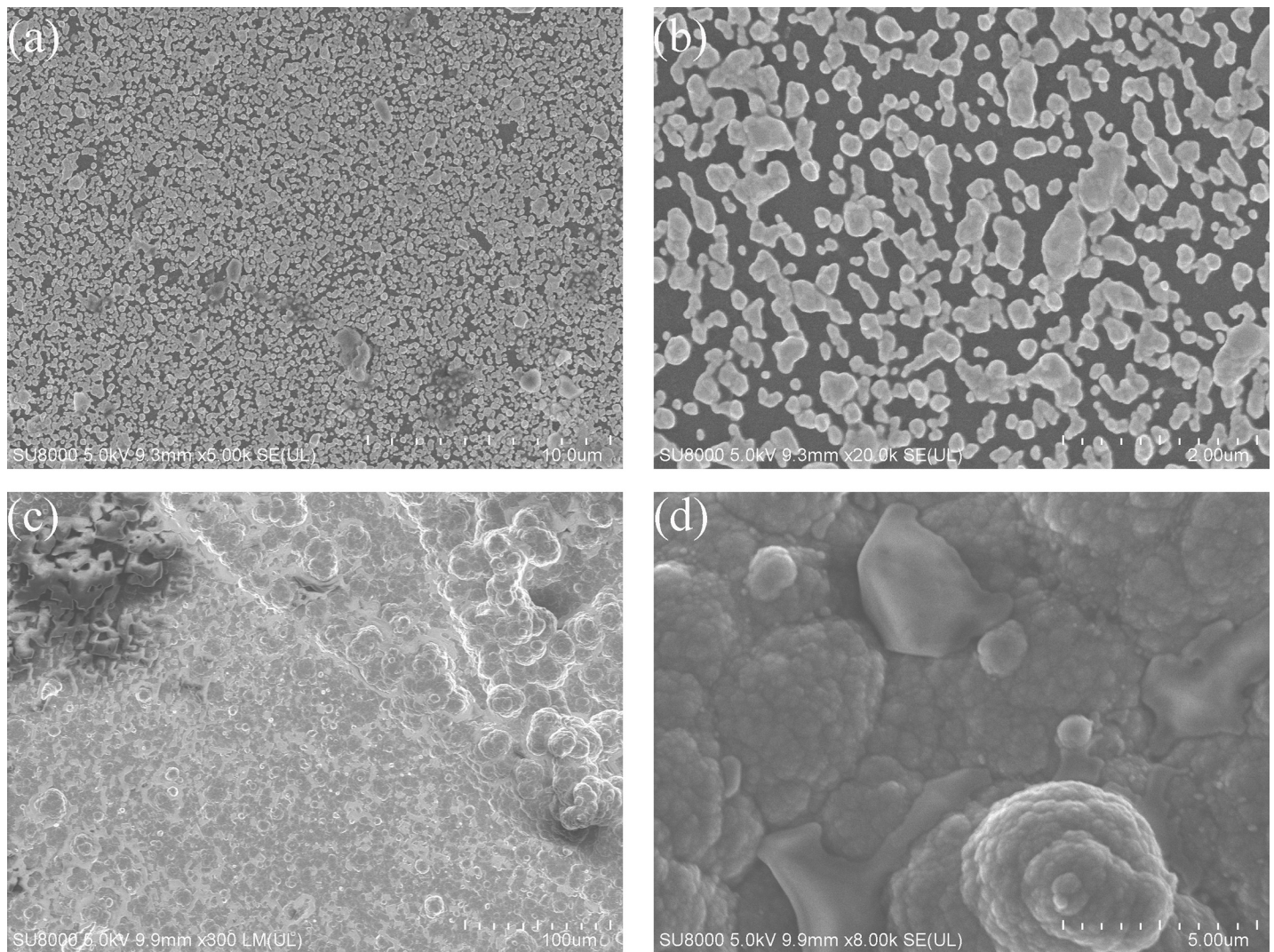


**Fig 7.** Representative FESEM images of microspheres for (a) AuNPs  $\times 5K$  (b) AuNPs  $\times 20K$  (c) PPY  $\times 300$  and (d) PPY  $\times 8K$ .

<https://doi.org/10.1371/journal.pone.0240173.g007>

this moment, the target ion NO<sub>3</sub><sup>-</sup> in the PPY sensitive membrane of the two electrodes was rapidly replaced by the interfering ion Cl<sup>-</sup>, which caused the change of the EMF. The potential of PPY/GCE went down obviously. After 30 minutes, the two electrodes were moved back to 0.1 mol/L NaNO<sub>3</sub> solution. The EMF of PPY/AuNPs/GCE fell back to the initial value rapidly and kept stable. Although the potential of PPY/GCE declined fast, it was not consistent with the initial value and existed a significant drift and responsive hysteresis. These results indicate that there is an interference environment known as the water layer between the sensitive membrane and GCE for PPY/GCE. The velocity of NO<sub>3</sub><sup>-</sup> replacing Cl<sup>-</sup> in the water layer is much smaller than the inverse process. Consequently, the final response potential cannot maintain stable and has serious drift. The changed composition of the water layer with the transport of the corresponding ions from samples which would diffuse through the PPY can affect the stability of potential seriously. However, the AuNPs solid contact layer can effectively inhibit the formation of interference water layer so as to keep stable potential of ISE. These results verify that a reduced water layer is formed between the solid contact layer of AuNPs and the PPY.

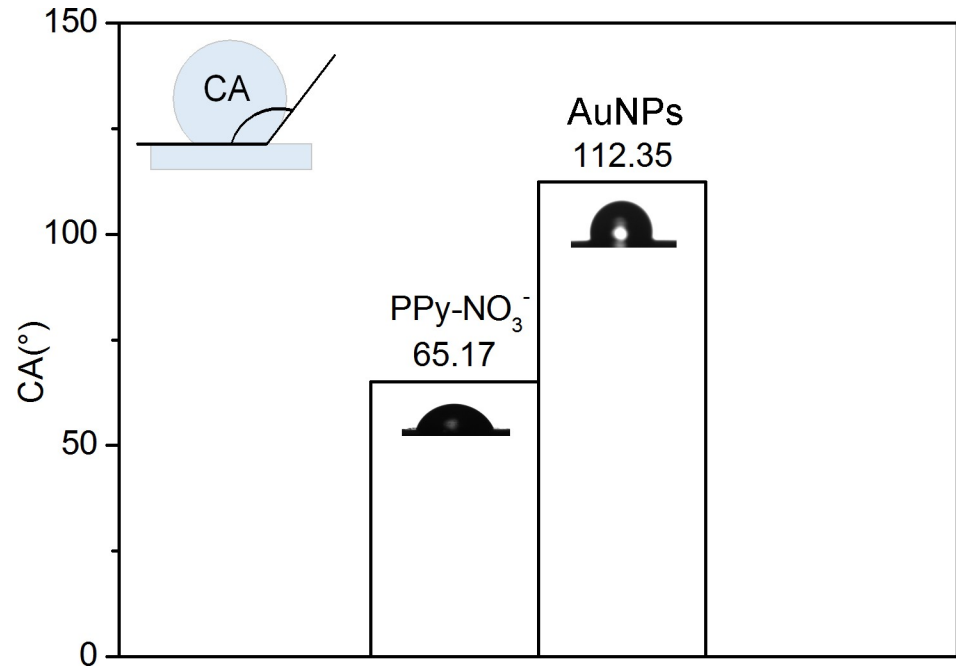


Fig 8. The comparison of contact angles in PPy-NO<sub>3</sub><sup>-</sup> membrane and in AuNPs solid contact layer.

<https://doi.org/10.1371/journal.pone.0240173.g008>

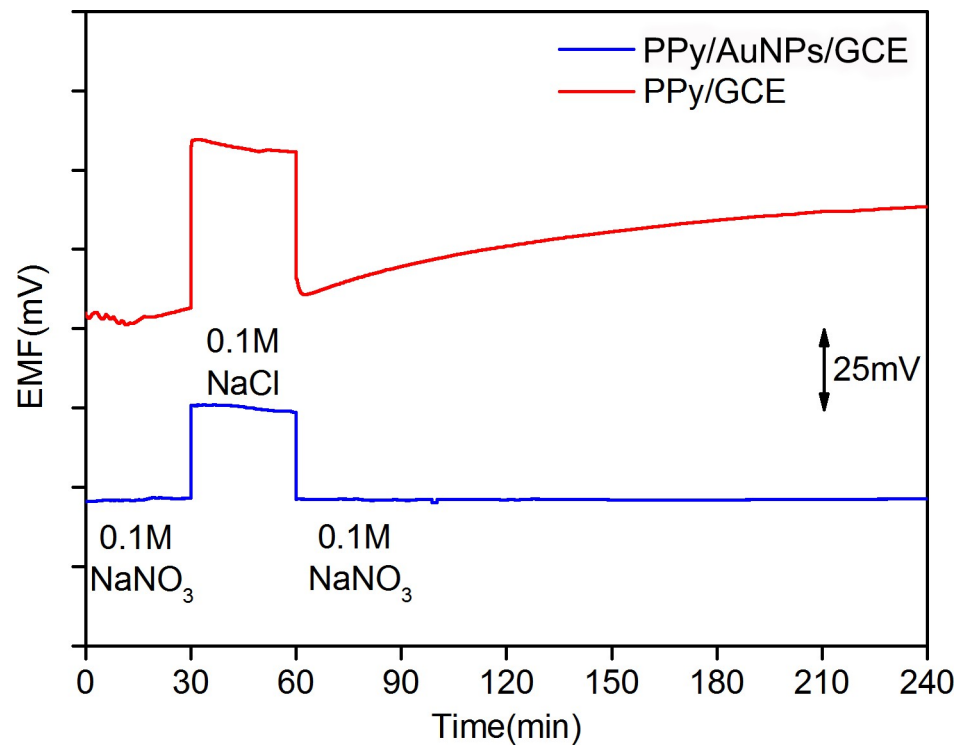
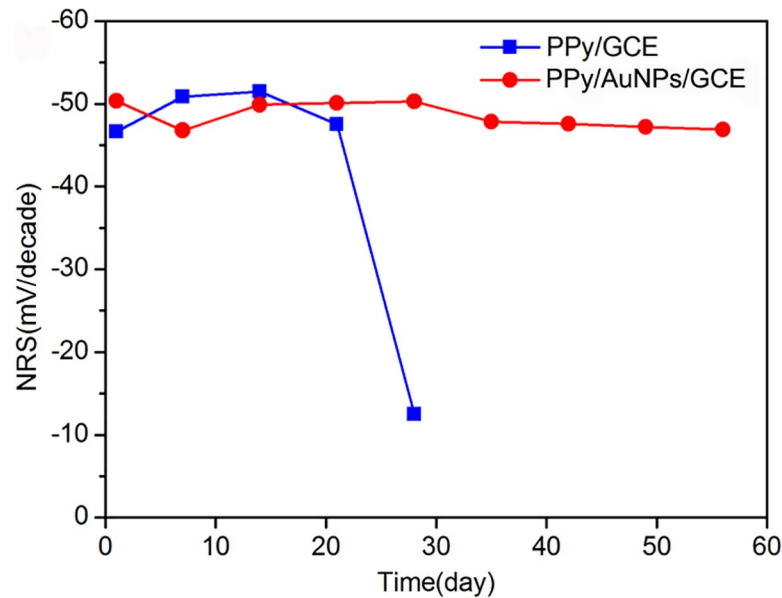


Fig 9. Water layer test of PPy/GCE and PPy/AuNPs/GCE.

<https://doi.org/10.1371/journal.pone.0240173.g009>



**Fig 10.** The lifetime test represented by NRS in the range of  $10^{-4}$  to  $10^{-1}$  mol/L.

<https://doi.org/10.1371/journal.pone.0240173.g010>

### Electrode lifetime

The EMFs of PPy/GCE and PPy/AuNPs/GCE were measured weekly in the gradient concentration NaNO<sub>3</sub><sup>-</sup> solution varying from  $10^{-4}$  to  $10^{-1}$  mol/L, then the NRSs were gotten by fitting calculation. As shown in Fig 10, in the range of  $10^{-4}$  to  $10^{-1}$  mol/L, the NRS of PPy/GCE was degraded extremely after 3 weeks. But the NRS of PPy/AuNPs/GCE was stable for 2 months. Therefore, the AuNPs solid contact layer can prolong the lifetime of NO<sub>3</sub><sup>-</sup> ASS-ISE.

### Comprehensive property and follow-up studies

The properties of the two electrodes (No.4 PPy/GCE and No.5 PPy/AuNPs/GCE) manufactured in this paper are compared with those in the literatures. As shown in Table 4, four indexes including NRS, LDL, response time and lifetime represent the performances of electrodes. No.6 has three better indexes, however its lifetime is so short that it cannot be applied in actual detection. Hence, the performances of No. 1 and No. 5 are superior. The lifetime of No.5 lasting for two months is twice that of No. 1, so PPy/AuNPs/GCE is more suitable for continuous detection of nitrogen concentration in nutrient solution.

In addition, the NRS and LDL of PPy/AuNPs/GCE can be improved further, and the AuNPs solid contact layer should be optimized to shield the water layer.

**Table 4.** Comparison of comprehensive performance for different electrodes.

| No. | Linear Range          | NRS<br>(mV/decade) | LDL<br>(mol/L)        | Response Time<br>(s) | Lifetime<br>(day) | Note          |
|-----|-----------------------|--------------------|-----------------------|----------------------|-------------------|---------------|
|     | (mol/L)               |                    |                       |                      |                   |               |
| 1   | $10^{-4}$ ~ $10^{-1}$ | -54.0              | $2.00 \times 10^{-5}$ | a few                | 30                | [38]          |
| 2   | $10^{-4}$ ~ $10^{-1}$ | -52.0              | $2.15 \times 10^{-5}$ | —                    | a few             | [39]          |
| 3   | $10^{-4}$ ~ $10^{-1}$ | -52.0              | $2.50 \times 10^{-5}$ | —                    | —                 | [40]          |
| 4   | $10^{-4}$ ~ $10^{-1}$ | -46.7              | $5.37 \times 10^{-5}$ | 6.875                | 21                | PPy/GCE       |
| 5   | $10^{-4}$ ~ $10^{-1}$ | -50.9              | $5.25 \times 10^{-5}$ | 0.45                 | 56                | PPy/AuNPs/GCE |
| 6   | $10^{-4}$ ~ $10^{-1}$ | -56                | $1.00 \times 10^{-6}$ | 62                   | 0.83              | [41]          |

<https://doi.org/10.1371/journal.pone.0240173.t004>

## Conclusions

In this work, an advanced and effective sensor based on AuNPs solid contact layer and molecularly imprinted polymer membrane was proposed and further used to fabricate the remarkably sensitive, selective and stable NO<sub>3</sub><sup>-</sup> ASS-ISE. Compared with the CWEs, the material preparation and technological process of ASS-ISE were simple. The performance of PPy/AuNPs/GCE was improved with high hydrophobic behavior in contrast to PPy/GCE, a reduced water layer is formed between the solid contact layer of AuNPs and the PPy. A NRS of -50.4 mV/decade in the linear range from 5.25×10<sup>-5</sup> to 10<sup>-1</sup> mol/L was obtained. The lifetime could reach 2 months. This work provides a useful approach for implementing AuNPs as solid contact layer in the ISEs, which could expand the applied scope of AuNPs fabricated sensing devices. The molecularly imprinted polymer membrane (PPy-NO<sub>3</sub><sup>-</sup> sensitive membrane) improves the disadvantages of PVC sensitive membrane. The better conductivity and stronger cohesive property can be attained.

## Author Contributions

**Methodology:** Lei Zhang, Pengcheng Liu.

**Supervision:** Zhengying Wei.

**Writing – original draft:** Lei Zhang.

**Writing – review & editing:** Lei Zhang, Pengcheng Liu.

## References

1. Savci S. An Agricultural Pollutant: Chemical Fertilizer. *International Journal of Environmental Science & Development*. 2012; 3(1).
2. Barak P, Jobe BO, Krueger AR, et al. Effects of long-term soil acidification due to nitrogen fertilizer inputs in Wisconsin. *Plant and soil*. 1997; 197(1): 61–69.
3. Nie P, Dong T, He Y, Qu F. Detection of soil nitrogen using near infrared sensors based on soil pretreatment and algorithms. *Sensors*. 2017; 17(5):1102.
4. Liu Y, Hu Z, Gao S, Günther D, Xu J, Gao C, et al. In situ analysis of major and trace elements of anhydrous minerals by LA-ICP-MS without applying an internal standard. *Chemical Geology*. 2008; 257(1–2):34–43.
5. Vakilian KA, Massah J. A farmer-assistant robot for nitrogen fertilizing management of greenhouse crops. *Computers and electronics in agriculture*. 2017; 139:153–63.
6. Cawse P. The determination of nitrate in soil solutions by ultraviolet spectrophotometry. *The Analyst*. 1967; 92(1094):311–5.
7. Fattahi N, Assadi Y, Hosseini MRM, Jahromi EZ. Determination of chlorophenols in water samples using simultaneous dispersive liquid–liquid microextraction and derivatization followed by gas chromatography-electron-capture detection. *Journal of Chromatography A*. 2007; 1157(1–2):23–9. <https://doi.org/10.1016/j.chroma.2007.04.062> PMID: 17512936
8. Voloschik IN, Litvina ML, Rudenko BA. Application of multi-dimensional liquid chromatography to the separation of some transition and heavy metals. *Journal of Chromatography A*. 1994; 671(1–2):205–209.
9. Bobacka J, Ivaska A, Lewenstam A. Potentiometric ion sensors. *Chemical reviews*. 2008; 108(2):329–51. <https://doi.org/10.1021/cr068100w> PMID: 18189426
10. Craggs A, Moody G, Thomas J. PVC matrix membrane ion-selective electrodes. Construction and laboratory experiments. *Journal of Chemical Education*. 1974; 51(8):541.
11. Cattrall R, Freiser H. Coated wire ion-selective electrodes. *Analytical chemistry*. 1971; 43(13):1905–6.
12. Freiser H. Coated wire ion-selective electrodes. *Ion-selective electrodes in analytical chemistry*: Springer; 1980. p. 85–105.
13. Janata J. *Principles of chemical sensors*: Springer Science & Business Media; 2010.
14. Otero T, de Larreta-Azelain E. Electrochemical generation of polythiophene films on platinum electrodes. *Polymer*. 1988; 29(8):1522–7.



15. Song RY, Park JH, Sivakkumar S, Kim SH, Ko JM, Park D-Y, et al. Supercapacitive properties of polyaniline/Nafion/hydrous RuO<sub>2</sub> composite electrodes. *Journal of power sources*. 2007; 166(1):297–301.
16. Watanabe M, Shirai H, Hirai T. Wrinkled polypyrrole electrode for electroactive polymer actuators. *Journal of Applied Physics*. 2002; 92(8):4631–7.
17. Soubiran P, Aeiyaç S, Lacaze P. Formation of polyparaphenylene (PPP) films by electrooxidation of biphenyl in CH<sub>2</sub>Cl<sub>2</sub>: A study of the nucleation process at a platinum electrode. *Journal of electroanalytical chemistry and interfacial electrochemistry*. 1991; 303(1–2):125–37.
18. Yin T, Qin W. Applications of nanomaterials in potentiometric sensors. *TrAC Trends in Analytical Chemistry*. 2013; 51:79–86.
19. Zeng X, Yu S, Yuan Q, Qin W. Solid-contact K<sup>+</sup>-selective electrode based on three-dimensional molybdenum sulfide nanoflowers as ion-to-electron transducer. *Sensors and Actuators B: Chemical*. 2016; 234:80–3.
20. Li J, Yin T, Qin W. An effective solid contact for an all-solid-state polymeric membrane Cd<sup>2+</sup>-selective electrode: Three-dimensional porous graphene-mesoporous platinum nanoparticle composite. *Sensors and Actuators B: Chemical*. 2017; 239:438–46.
21. Yuan D, Anthis AH, Ghahraman Afshar M, Pankratova N, Cuartero M, Crespo GnA, et al. All-solid-state potentiometric sensors with a multiwalled carbon nanotube inner transducing layer for anion detection in environmental samples. *Analytical chemistry*. 2015; 87(17):8640–5. <https://doi.org/10.1021/acs.analchem.5b01941> PMID: 26272001
22. Yu K, He N, Kumar N, Wang N, Bobacka J, Ivaska A. Electrosynthesized polypyrrole/zeolite composites as solid contact in potassium ion-selective electrode. *Electrochimica Acta*. 2017; 228:66–75.
23. Yang G, Chang Y, Yang H, Tan L, Wu Z, Lu X, et al. The preparation of reagentless electrochemical immunosensor based on a nano-gold and chitosan hybrid film for human chorionic gonadotrophin. *Analytica chimica acta*. 2009; 644(1–2):72–7. <https://doi.org/10.1016/j.aca.2009.04.021> PMID: 19463565
24. Ling S, Yuan R, Chai Y, Zhang T. Study on immunosensor based on gold nanoparticles/chitosan and MnO<sub>2</sub> nanoparticles composite membrane/Prussian blue modified gold electrode. *Bioprocess and bio-systems engineering*. 2009; 32(3):407–14. <https://doi.org/10.1007/s00449-008-0260-2> PMID: 18923847
25. Zhuo Y, Yuan R, Chai Y, Tang D, Zhang Y, Wang N, et al. A reagentless amperometric immunosensor based on gold nanoparticles/thionine/Nafion-membrane-modified gold electrode for determination of  $\alpha$ -1-fetoprotein. *Electrochemistry communications*. 2005; 7(4):355–60.
26. Nagar B, Balsells M, de la Escosura-Muñiz A, et al. Fully printed one-step biosensing device using graphene/AuNPs composite[J]. *Biosensors and Bioelectronics*, 2019, 129: 238–244. <https://doi.org/10.1016/j.bios.2018.09.073> PMID: 30279057
27. Liang P, Canoura J, Yu H, et al. Dithiothreitol-regulated coverage of oligonucleotide-modified gold nanoparticles to achieve optimized biosensor performance[J]. *ACS applied materials & interfaces*, 2018, 10(4): 4233–4242.
28. Silva, Nádia F.D, Magalhães, Júlia M.C.S, Barroso, Fátima M., et al. In situ formation of gold nanoparticles in polymer inclusion membrane: Application as platform in a label-free potentiometric immunosensor for Salmonella typhimurium detection[J]. *Talanta*, 2019, 194:134–142. <https://doi.org/10.1016/j.talanta.2018.10.024> PMID: 30609512
29. Liu Y, Liu Y, Yan R, et al. Bimetallic AuCu nanoparticles coupled with multi-walled carbon nanotubes as ion-to-electron transducers in solid-contact potentiometric sensors[J]. *Electrochimica Acta*, 331.
30. Fakhari AR, Raji TA, Naeimi H. Copper-selective PVC membrane electrodes based on salens as carriers. *Sensors and Actuators B: Chemical*. 2005; 104(2):317–23.
31. Bakker Eric, Bühlmann Philippe, Pretsch Ernö. *Polymer Membrane Ion-Selective Electrodes—What are the Limits?*[J]. *Electroanalysis*, 2015, 11(13):915–933.
32. Gupta VK, Singh AK, Mehtab S, Gupta B. A cobalt (II)-selective PVC membrane based on a Schiff base complex of N, N'-bis (salicylidene)-3, 4-diaminotoluene. *Analytica chimica acta*. 2006; 566(1):5–10.
33. Zamani H, Rajabzadeh G, Firouz A, Ganjali M. Determination of copper (II) in wastewater by electroplating samples using a PVC-membrane copper (II)-selective electrode. *Journal of Analytical Chemistry*. 2007; 62(11):1080–7.
34. Haupt K, Mosbach K. Molecularly imprinted polymers and their use in biomimetic sensors. *Chemical reviews*. 2000; 100(7):2495–504. <https://doi.org/10.1021/cr990099w> PMID: 11749293
35. Mikhelson KN. *Ion-selective electrodes*: Springer; 2013.
36. Gabriel S, Cécius M, Fleury-Frenette K, Cossement D, Hecq M, Ruth N, et al. Synthesis of adherent hydrophilic polypyrrole coatings onto (semi) conducting surfaces. *Chemistry of materials*. 2007; 19(9):2364–71.

37. Liu L, Liu J, Bo G, Yang F, Crittenden J, Chen Y. Conductive and hydrophilic polypyrrole modified membrane cathodes and fouling reduction in MBR. *Journal of membrane science*. 2013; 429:252–8.
38. Mourzina YG, Ermolenko YE, Yoshinobu T, Vlasov Y, Iwasaki H, Schöning MJ. Anion-selective light-addressable potentiometric sensors (LAPS) for the determination of nitrate and sulphate ions. *Sensors and Actuators B: Chemical*. 2003; 91(1–3):32–8.
39. Zhen RG, Smith SJ, Miller AJ. A comparison of nitrate-selective microelectrodes made with different nitrate sensors and the measurement of intracellular nitrate activities in cells of excised barley roots. *Journal of Experimental Botany*. 1992; 43(2):131–8.
40. Högg G, Steiner G, Cammann K. Development of a sensor card with integrated reference for the detection of nitrate. *Sensors and Actuators B: Chemical*. 1994; 19(1–3):376–9.
41. Hara H, Ohkubo H, Sawai K. Nitrate ion-selective coated-wire electrode based on tetraoctadecylammonium nitrate in solid solvents and the effect of additives on its selectivity. *The Analyst*. 1993; 118(5):549–52.